# Decreasing the error probability in optical transmission lines

C. Fidani and P. Tombesi
*Dipartimento di Matematica e Fisica, Università di Camerino and INFM, Camerino via Madonna delle Carceri 62032 Camerino, Italy*
(Received 1 March 2001; published 20 February 2002)

We show that, for a continuous-wave input, the error probability, of bit transmission along a third-order nonlinear line with high nonlinearity, might decrease even below its input value. Quantum fluctuations are handled by means of the Wigner function. The resulting evolution equation is exactly solved with the Green-function method, which permits to calculate the density-matrix elements.

DOI: 10.1103/PhysRevA.65.033815 PACS number(s): 42.50.Ct, 42.65.Sf, 03.67.Hk, 42.50.Dv

## I. INTRODUCTION

A wide variety of phenomena both classical [1] and quantum [2] are produced by the interaction of the electromagnetic field with a nonlinear medium. These phenomena can be used for information manipulation and transmission [3]. In order to transmit bit codified information down an optical fiber, one should be able to control the error probability. This is a measurement of error in codified information of the receiver and gives a measure of the message quality at a given distance from the sender. The optimal goal would be not only controlling it but to have the possibility of reducing the error probability. The error probability in a measurement may have classical and quantum origins. From the classical point of view the efficiency of detector, the thermal fluctuations, the absorption, and the dispersion are the principal causes. From the quantum point of view fluctuations are the principal cause. The detector efficiency and the dispersion are not considered in this paper while the thermal fluctuations are very small for optical signals. We are concerned with absorption and quantum fluctuations effects on the error probability.

The squeezed states in quantum optics, have the peculiarity that the quadrature noise of the electromagnetic field in these states is reduced below the shot noise level [4]. Squeezed states can be obtained with a nonlinear interaction between field and matter. With second-order optical nonlinear media the squeezed state is generated by a parametric amplification of the signal, at the expenses of a more intense pump field [5]. As a result one of the signal quadratures together with its fluctuations is amplified while the orthogonal quadrature with its fluctuations is deamplified or squeezed. The error probability is, in this case, strictly linked to the signal-to-noise ratio (SNR) that remains constant for both quadratures and, therefore, also the error probability remains constant.

The principal goal of this paper is to use third-order nonlinearities. In this case the SNR is enhanced because the signal amplitude remains practically unchanged and the noise is squeezed, however, the error probability is not strictly linked to the SNR as it will become clear below.

Even with the modern technology of materials [6] the entity of the $\chi^{(3)}$ nonlinearity is still too small, however, a number of applications were already realized [7] by using laser sources that have a quasimonochromatic radiation with high photon flux. Since the coupling depends on the intensity, one obtains a stronger nonlinear coupling that permits the observation of quantum effects [8]. Novel schemes for obtaining high third-order nonlinearity were recently proposed. They are based on the electromagnetically induced transparency (EIT) [9,10] or on the cascading nonlinearity in $\chi^{(2)}$ media [11,12]. In EIT the high nonlinearity is obtained in resonance conditions in four-level systems by using the absorbing destructive interference, combined with the constructive interference of the nonlinear susceptibility [10]. The experiment in ultracold sodium atom gas showed a velocity propagation of light many orders of magnitude smaller than the light propagation in vacuum. The phase-shift measurement allowed to obtain big values of optical nonlinearity even with very small photon flux [13]. Moreover, experiments with warm atomic gas were also reported [14], showing the possibility of high nonlinearities in nonextreme conditions. The high nonlinearities in those media could hardly be considered useful for transmission lines, however. In currently available optical fibers the third-order nonlinearity, although present, is very small. Nevertheless, it could be enhanced by appropriately doping the fiber in nonlinear periodic core waveguides [15].

We shall use such nonlinearities in order to show that the error probability can be diminished depending upon the measurement typology and on the observable to be measured. It will become clear below that, with a high third-order nonlinearity with respect to the absorption, the error probability of bits transmission could, in principle, be reduced even below the input value.

The paper is organized as follows; in Sec. II the error probability is introduced, then it is calculated for the Gaussian distribution and for a second-order nonlinear line as an example, in this case it is directly linked to the SNR. In Sec. III the model for a third-order nonlinear line is described and the error probability calculated, then the decreasing of error probability is shown to be a different quantum phenomenon with respect to the squeezing. Section IV is devoted to the long haul transmission showing the gain of nonlinear lines with respect to the linear ones. The conclusions are in Sec. V. Sketches of all the cumbersome calculations are reported in five Appendices.

## II. THE ERROR PROBABILITY

To this purpose we shall refer to homodyne measurements of the signal quadrature.

 

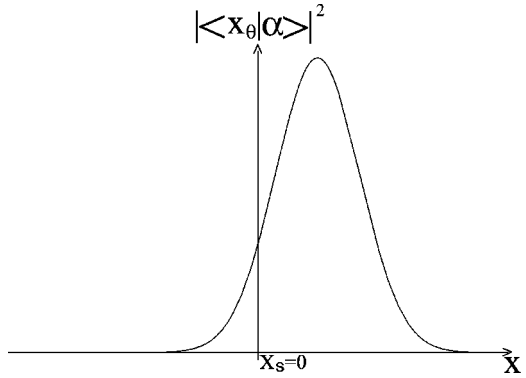


FIG. 1. The error probability is the area under the tail of the Gaussian probability distribution, where the tail is the part of distribution on the left side of the decision threshold $X_s=0$.

$$X_\theta=\frac{ae^{-i\theta}+a^+e^{i\theta}}{2}, \tag{1}$$

where the phase $\theta$ is controlled by the experimenter with the local oscillator. The probability amplitude of a homodyne measurement of the quadrature $X_\theta$ on a coherent state is obtained by [16]

$$\langle\alpha|X_\theta\rangle=\sum_{n=0}^{\infty}\langle\alpha|n\rangle\langle n|X_\theta\rangle = \sqrt[4]{\frac{2}{\pi}}\exp\left[-x^2+2x\alpha^*e^{i\theta}-\frac{|\alpha|^2}{2}-\frac{\alpha^{*2}}{2}e^{2i\theta}\right], \tag{2}$$

where $|\alpha\rangle=|re^{i\varphi}\rangle$ represents the coherent state with average number of photons $r^2$ and phase $\varphi$. The eigenvalue of the quadrature operator defined in Eq. (1) is $x$, with $X_\theta|X_\theta\rangle=x|X_\theta\rangle$. The probability distribution is then the Gaussian

$$|\langle X_\theta|\alpha\rangle|^2=\sqrt{\frac{2}{\pi}}\exp\{-2[x-r\cos(\theta-\varphi)]^2\}. \tag{3}$$

In a digital measurement, which uses the homodyne measurement of the signal quadrature , the bits ''0,1'' are, respectively, given by the negative and positive values of $x$ [17]. The area under the Gaussian distribution for positive values of $x$ represents the success probability in the measurement of the bit ''1'' while the area under the negative part of $x$ represents the success probability on the measure of the bit ''0.'' The point $x=0$ represents the decision threshold. During the transmission of the bit ''1'' the Gaussian probability distribution has a positive mean value, Fig. 1, so the error probability is just the area of the distribution tail for $x\leqslant 0$ and can be calculated with the error function [18]. Decreasing the error probability is extremely important in optical digital transmission systems. This is relevant for long haul transmission, but for very short haul as well. In that they are the only sufficiently fast media for information exchange among computers or the various subsections of a given computer.

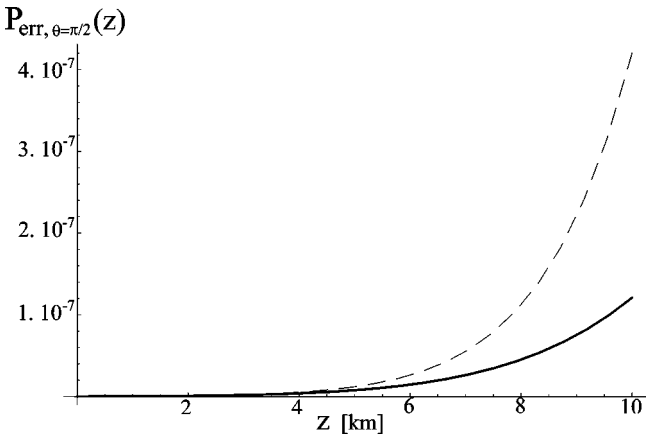


FIG. 2. The error probability in a driven $\chi^{(2)}$ nonlinear transmission line (continuous line) increases very slowly with respect to the linear case (dashed line). Here $r_o^2=10$ and $\gamma/c=5\times10^{-5}$ m$^{-1}$.

Because of its Gaussian character the probability distribution (3) can be expressed in terms of SNR [18], showing that the success probability degrades with SNR. That is because, due to absorption, the field amplitude diminishes. The noise, indeed, does not grow because the thermal-photon contribution to the total photon number is negligible at optical frequencies. To estimate such a degradation, as function of the various parameters of the transmission line and the field, we start from the SNR [19]. In optical transmission lines of length $z$ with absorption $\bar{\gamma}$ the quadrature amplitude is $\langle X_\theta(z)\rangle=r\cos(\theta-\varphi)e^{-\bar{\gamma}z/2}$ and the variance, neglecting the thermal contribution, is $\Delta X_\theta^2(z)=\langle X_\theta^2(z)\rangle-\langle X_\theta(z)\rangle^2=1/4$ then

$$\mathcal{R}_\theta(z)=\frac{\langle X_\theta(z)\rangle^2}{\Delta X_\theta^2(z)}=4r^2\cos^2(\theta-\varphi)e^{-\bar{\gamma}z}, \tag{4}$$

where $\mathcal{R}$ is the signal-to-noise ratio. The error probability exponentially decays with the line length, Fig. 2, and can be obtained [18] by the error function,

$$P_{err,\theta}(z)=\frac{1-\mathrm{erf}[\sqrt{2}r\cos(\theta-\varphi)e^{-\bar{\gamma}z/2}]}{2}. \tag{5}$$

The enhancement of error probability with the line length can be understood by considering the distribution (3), one observes that the Gaussian distribution is shifted by $r(1-e^{-\bar{\gamma}z/2})\cos(\theta-\varphi)$ toward the origin,

$$|\langle X_\theta|\alpha e^{-\bar{\gamma}z/2}\rangle|^2=\sqrt{\frac{2}{\pi}}e^{-2[x-re^{-\bar{\gamma}z/2}\cos(\theta-\varphi)]^2}, \tag{6}$$

thus, the area under the tail of the Gaussian for $x<0$ grows. In a recent paper [19], following the Caves and Crouch approach [20], it has been shown how it could be possible that the degradation of SNR becomes weaker along an optical transmission line with second-order nonlinearity. It is obtained with a mixing of three fields (in, out, and driving) and one obtains a parametric amplification of the signal along the

line with squeezing of losses at the same time. By assuming that the parametric amplification exactly compensates the loss it was shown that SNR of the $\theta=\pi/2$ quadrature decreases in a weaker way with the propagation length,

$$\mathcal{R}_{\pi/2}(z)=\frac{4r^2\sin^2\varphi}{1+\overline{\gamma}z}, \tag{7}$$

The result gives a less evident enhancement of the error probability, Fig. 2 (continuous line),

$$P_{err,\pi/2}(z)=\frac{1}{2}\left(1-\mathrm{erf}\left[\frac{\sqrt{2}r\sin\varphi}{\sqrt{1+\overline{\gamma}z}}\right]\right). \tag{8}$$

The technology is not yet mature to produce transmission lines with second-order nonlinearity. Furthermore, neither the parametric amplification nor the above quoted configuration are able to decrease the error probability. Indeed, the parametric amplification preserves the error probability because it preserves the SNR while the above configuration just slows down its growing. We have already quoted that optical media with third-order nonlinearity may produce an anisotropic distribution of fluctuations in phase and a relevant degree of squeezing can be obtained for given values of various parameters [21–25]. The effect of this interaction on the signal is to enhance the SNR that, however, is obtained only after given and well-defined propagation lengths and measuring particular quadratures. By measuring these quadratures, however, the probability distribution is no more Gaussian and the error probability is no more easily connected with the SNR, otherwise one could surely affirm that the error probability will decrease. That is why, one has to carefully consider its behavior.

### III. THE MODEL

In the following the absorption of fluctuations along the line will be described with the cavity model. The system's evolution is then described by the master equation of a cavity with loss and nonlinear interaction. The equations of motion for the boson operator $a$ of the propagating mode, in interaction picture, is also obtainable from the ''beam splitter'' model (see Appendix A) used by Caves and Crouch [20]. It is equivalent to that obtained with the cavity model, setting $t=z/c$,

$$\frac{da(t)}{dt}=-\frac{\gamma}{2}a(t)-i\chi a^+(t)a^2(t)+\sqrt{\gamma}a_{ns}(t), \tag{9}$$

with

$$\langle a_{ns}\rangle=\langle a_{ns}^+\rangle=0,\quad \langle a_{ns}^+a_{ns}\rangle=\langle a_{ns}a_{ns}^+\rangle-1=\overline{n},$$
$$\langle a_{ns}a_{ns}\rangle=\langle a_{ns}^+a_{ns}^+\rangle=0, \tag{10}$$

representing the noise correlations and $\overline{n}$ gives the mean thermal photon number, which at optical frequencies can be considered vanishingly small. This is a nonlinear quantum stochastic operator equation. In order to obtain a solution of our problem we shall reconsider it in terms of the coherent states representation of the density matrix $\hat{\rho}$ [26]. For one cavity mode with a Kerr nonlinearity in presence of loss and in the interaction picture, we get [21]

$$\frac{\partial\hat{\rho}}{\partial t}=-\frac{i}{\hbar}[\hat{H}_I,\hat{\rho}]+\frac{\gamma}{2}(2a\rho a^+-a^+a\rho-\rho a^+a), \tag{11}$$

where

$$\hat{H}_I=\hbar\chi(a^+)^2a^2 \tag{12}$$

is the interaction Hamiltonian. Assuming that the initial state is a coherent state $|\alpha_0\rangle$, at time $t$ it will be $|\Psi(t)\rangle$. The probability distribution of a quadrature $\theta$ measurement, $|\langle X_\theta|\Psi(t)\rangle|^2$, can be obtained from the density matrix [26]. One cannot use, however, the Glauber $P$-representation because it becomes extremely singular [2] with the $\chi^{(3)}$ nonlinearity. Using the overcompleteness of the coherent states the probability distribution can be written as

$$|\langle X_\theta|\Psi(t)\rangle|^2=\int\int\frac{d^2\alpha_1}{\pi}\frac{d^2\alpha_2}{\pi}\langle X_\theta|\alpha_1\rangle\langle\alpha_1|\hat{\rho}(t)|\alpha_2\rangle\times\langle\alpha_2|X_\theta\rangle, \tag{13}$$

where the expectation value of the density matrix can be expressed in terms of the Wigner function as shown by Cahill and Glauber [26],

$$\langle\alpha_1|\hat{\rho}(t)|\alpha_2\rangle=\int d^2\alpha W(\alpha,t)2\langle\alpha_1|\alpha_2\rangle\times\exp[-2(\alpha_1^*-\alpha^*)(\alpha_2-\alpha)], \tag{14}$$

with $\langle\alpha_1|\alpha_2\rangle=\exp(-|\alpha_1|^2/2-|\alpha_2|^2/2+\alpha_2\alpha_1^*)$. The equation of motion of the density matrix is equivalent to the equation of motion for the Wigner function that is not singular with a Kerr nonlinearity. By standard methods [26,27] and transforming in polar coordinates, we get

$$\frac{\partial}{\partial t}W(r,\varphi,t)=\frac{1}{2}\left\{\gamma\left(\frac{\partial}{\partial r}r+1\right)+\left(\gamma-\frac{\chi}{2}\frac{\partial}{\partial\varphi}\right)\Delta+2\chi(r^2-1)\frac{\partial}{\partial\varphi}\right\}W(r,\varphi,t), \tag{15}$$

where $\Delta$ represents the Laplacian operator in polar coordinates. The solution of this equation can be obtained by using the method of Kartner and Schenzle [27], which consists in calculating the Green function, and the Wigner function in $z=ct$ is obtained in the usual way, once its initial value is given,

$$W(r,\varphi,t)=\int_0^{2\pi}\int_0^\infty G(r,\varphi,t;r',\varphi',0)W(r',\varphi',0)r'dr'd\varphi'. \tag{16}$$

Following [27] we obtain the Green function, the Wigner function, and the probability distribution (see Appendix B), which are, respectively, given by the following expressions:

$$G(r,\varphi,t;r',\varphi',0)=\frac{1}{\pi}\sum_{m=-\infty}^{\infty}\frac{2\beta_m\exp[im(\varphi-\varphi'-\chi t)+\gamma t/2]}{(\gamma+\beta_m)\sinh(\beta_m t/2)}I_m[4rr'\beta_m/(\gamma+\beta_m)\sinh^{-1}(\beta_m t/2)]$$
$$\times\exp\left[-\frac{2\beta_m(r^2+r'^2)}{\gamma+\beta_m}\coth(\beta_m t/2)-\frac{2\gamma(r^2-r'^2)}{\gamma+\beta_m}\right], \tag{17}$$

$$W(\alpha,t)=\frac{2}{\pi}\exp[-2|\alpha_0|^2-2|\alpha|^2]\sum_{m=-\infty}^{\infty}I_m[4|\alpha_o||\alpha|e^{-\beta_m t/2}]\exp\left[im\left(\varphi-\varphi_o+\frac{\chi t}{2}\right)-|\alpha_o|^2(e^{-\beta_m t}-1)\left(1+\frac{\gamma}{\beta_m}\right)\right], \tag{18}$$

$$\langle\alpha_1|\hat{\rho}(t)|\alpha_2\rangle=\exp[-|\alpha_1|^2/2-|\alpha_2|^2/2]\sum_{m=-\infty}^{\infty}\left(\frac{\alpha_2}{\alpha_1^*}\right)^{|m|/2}I_m[2|\alpha_o|\sqrt{\alpha_1^*\alpha_2}e^{-\beta_m t/2}]$$
$$\times\exp\left\{-im\left(\varphi_o+\frac{\chi t}{2}\right)-|\alpha_o|^2\left[\frac{\gamma e^{-\beta_m t}-im\chi}{\beta_m}\right]\right\}, \tag{19}$$

$$|\langle X_\theta|\Psi(t)\rangle|^2=\sqrt{\frac{2}{\pi}}e^{-2x^2}\sum_{n,k=0}^{\infty}\left(\frac{|\alpha_o|^2e^{-\beta_{n-k}t}}{2}\right)^{(n+k)/2}\frac{H_n[\sqrt{2}x]}{n!}\frac{H_k[\sqrt{2}x]}{k!}$$
$$\times\exp\left[i(k-n)\left(\varphi_o-\theta+\frac{\chi t}{2}\right)\right]\exp\left\{-|\alpha_o|^2\left[\frac{\gamma e^{-\beta_{n-k}t}-i(n-k)\chi}{\beta_{n-k}}\right]\right\}, \tag{20}$$

where $\beta_m=\gamma-im\chi$. $I_m$ represents the modified Bessel function [28] and $|\alpha_o\rangle=|r_o e^{i\varphi_o}\rangle$ is the initial coherent state. When $\chi=0$ the probability distribution coincides with the Gaussian in Eq. (6). The error probability is obtained by integrating Eq. (20) along the negative semiaxis if the bit ''1'' was sent. One gets the following expression (see Appendix C):

$$P_{err,\theta}(t)=\int_{-\infty}^{0}dx|\langle X_\theta|\Psi(t)\rangle|^2=\frac{1}{2}-\sqrt{\frac{2}{\pi}}|\alpha_o|e^{-\gamma t/2}\sum_{m=1/odd}^{\infty}\mathrm{Re}\left[\frac{I_{(m-1)/2}[-|\alpha_o|^2e^{-\beta_m t}]-I_{(m+1)/2}[-|\alpha_o|^2e^{-\beta_m t}]}{m}\right.$$
$$\left.\times\exp\left\{im(\theta-\varphi_o)-|\alpha_o|^2\left(\frac{\gamma e^{-\beta_m t}-im\chi}{\beta_m}\right)\right\}\right], \tag{21}$$

where $m$ takes only odd integer values and Re represents the real part. Notice that the result would be the same if the bit ''0'' were sent. Indeed, integrating Eq. (20) along the positive semiaxis for the transmission of a bit ''0,'' it should be shifted by $\pi$.

Let us first substitute in the above equation $t=z/c$ and fix the values of parameters $\gamma$ and $\chi$. The ratio between the two parameters is critical to observe quantum effects. In fact, the first destroys the coherence effects produced by the second. In a practical situation of a fiber having losses of 0.2 dB/km, in which the input is a coherent state of mean photon number $|\alpha_o|^2=r_o^2=10$, the effective nonlinear coefficient $\chi/c$ must be of the same order of the absorption coefficient for observing quantum effects. The absorption coefficient is $\gamma/c$ and corresponds to about $5\times10^{-5}$ m$^{-1}$ for the above fiber. Eq. (21) is plotted in Figs. 3 and 4 for the absolute minimum of the error probability. In Fig. 3 it is plotted for several ratios $\chi/\gamma$ setting $\theta=\theta_m$. In Fig. 4 $z_m=609\,m$ with $\chi/\gamma=1$ is shown, where $z_m$ is the coordinate of the lower minimum, and $\theta$ represents the quadrature angle. In these figures the dashed-dotted horizontal lines represent the initial error probability, that is the one of the input quadrature $\theta=0$. The continuous dark lines represent the error probability Eq. (21), where the sum is taken up to $m=53$ since for $m>53$ the terms of the sum give very small contributions. The error probability obtained with a linear medium with absorption $\gamma/c$ is represented by the dashed lines. The obtained minima show that the third-order nonlinearity can reduce the error probability below the one obtained with the usual linear fiber and the same absorption coefficient. Furthermore, with a bigger ratio $\chi/\gamma$ it could become smaller than the initial error probability, see Fig. 3 with $\chi/\gamma=1.4$ and 10. Let us now comment about the connection of this result with squeezing. It is possible to show that the length at which one obtains the minimum of error probability does not coincide with that of the maximum obtainable squeezing. Indeed, for example, in the case of $\chi/\gamma=10$ we get $z_m=60m$ for the minimum of error probability observing the quadrature $\theta=20°$, while the maximum squeezing is obtainable at $z=126m$. In our case the squeezing is, of course, present but its value is always

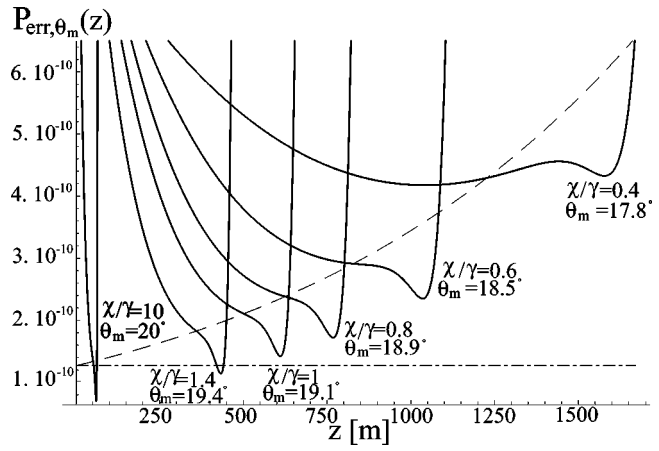


FIG. 3. The length-dependent error probability in a third-order nonlinear transmission line (continuous lines) for various ratio of $\chi/\gamma$, with fixed local-oscillator phase ($\theta=\theta_m$) of the homodyne detector. Here $r_o^2=10$ photons and $\gamma/c=5\times10^{-5}$ m$^{-1}$. The values of the minima are smaller than those corresponding to the error probability of a linear line (dashed line). If the ratio $\chi/\gamma>1$ then the error probability can go below the initial level (horizontal dashed-dotted line) with an apparent paradoxical increase of information.

smaller than 48% at the distance where the error probability gets its minimum. The maximum obtainable squeezing at $z=126m$ is about 60%. The two phenomena appear different, although connected because both are consequences of Kerr nonlinearities.

The base10 logarithm of the ratio between the error probability in the nonlinear medium and the linear one is plotted in Fig. 5. It is evident that the bigger the $\chi/\gamma$ ratio the smaller the minimum. Then, defining the ''error factor,''

$$\mathcal{E}=10\log_{10}[P_{err}(\text{out})/P_{err}(\text{in})] \tag{22}$$

in decibel, we can plot the error factor vs $z$ and compare the linear and nonlinear transmission lines with the same initial error probability $P_{err}(\text{in})$,

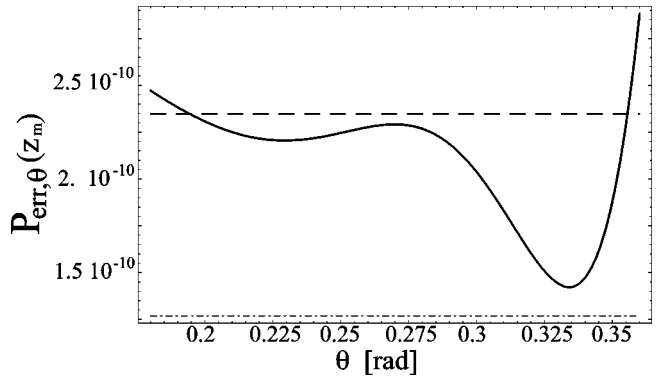


FIG. 4. The phase quadrature of the error probability in a third-order nonlinear transmission line (continuous line) for a fixed length $z=z_m=609m$ with $r_o^2=10$ and $\gamma/c=\chi/c=5\times10^{-5}$ m$^{-1}$. The value of the error probability after the same length of a linear medium with $\theta=0$ is the horizontal dashed line. The horizontal dashed-dotted line with $\theta=0$ represents the error probability of the input signal.

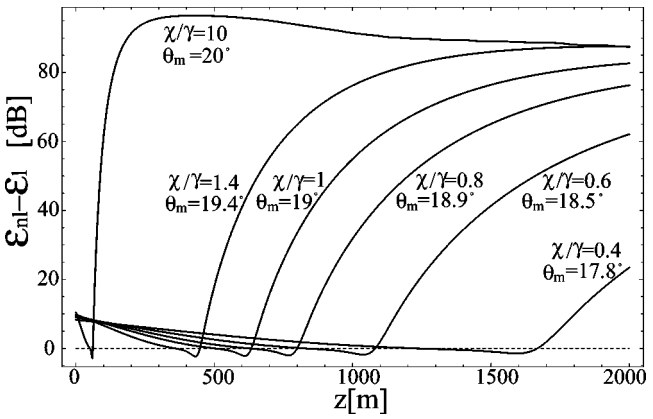


FIG. 5. The plots show the improvement of the error probability for various $\chi/\gamma$ ratios by the best phase measurement. The best error probability is when $\epsilon_{nl}-\epsilon_l\leqslant0$. We observe that this improvement increases with $\chi/\gamma$, but it is always $P_{err,nl}/P_{err,l}\geqslant1/2$.

$$\mathcal{E}_{nl}-\mathcal{E}_l=10\log_{10}[P_{err,nl}(\text{out})/P_{err,l}(\text{out})]. \tag{23}$$

In Fig. 5 the continuous line is $\mathcal{E}_{nl}-\mathcal{E}_l$ while the dashed line corresponds to the input error factor. It is possible to show that always is $P_{err,nl}/P_{err,l}\geqslant1/2$, thus $\mathcal{E}_{nl}-\mathcal{E}_l\geqslant-3dB$ for a third-order nonlinearity. It means that the error factor for a nonlinear line could be smaller than the linear one but the difference between them is limited by 3 dB. The value of the input error probability chosen is $P_{err,0}(0)=1.27\times10^{-10}$. With the usual linear transmission line it becomes $P_{err,l}(z_m)=1.35\times10^{-10}$, while with the nonlinear medium with the same absorption at the same distance becomes $P_{err,nl}(z_m)=7\times10^{-11}$ for $\theta_m\simeq19°$. This result could appear odd if one calculates the information losses in such a channel [18]. Indeed, it would result an enhancement of information with the propagation length. This apparent oddness derives from the channel definition, which is strictly connected with the measurement scheme used. The homodyne measurement only selects one signal quadrature while the information is on all quadratures; that is on the whole phase space of the field. One can understand that the effect of the third-order nonlinearity is to redistribute the information on the phase space with an enhancement of information in some signal quadratures and a consequent loss of information in others. If we, however, consider the total entropy $S(t)=-K_B\text{Tr}[\hat{\rho}(t)\ln\hat{\rho}(t)]$, which is shown in Appendix D, ($K_B$ is the Boltzman constant) we obtain that it grows as it should. In Fig. 6 the entropy,

$$\begin{aligned}S(t)=-K_B\{&[\text{Tr}\,\hat{\rho}^2(t)-1]-[\text{Tr}\,\hat{\rho}^3(t)-2\,\text{Tr}\,\hat{\rho}^2(t)+1]/2\\&+[\text{Tr}\,\hat{\rho}^4(t)+3\text{Tr}\hat{\rho}^3(t)+3\,\text{Tr}\,\hat{\rho}^2(t)-1]/3+\cdots\},\end{aligned} \tag{24}$$

is plotted considering the first two terms of the series, since the next terms are much smaller. Thus, the total information summed on all signal quadratures will decrease. This is what one should expect because the loss absorbs part of the signal irreversibly destroying part of information.

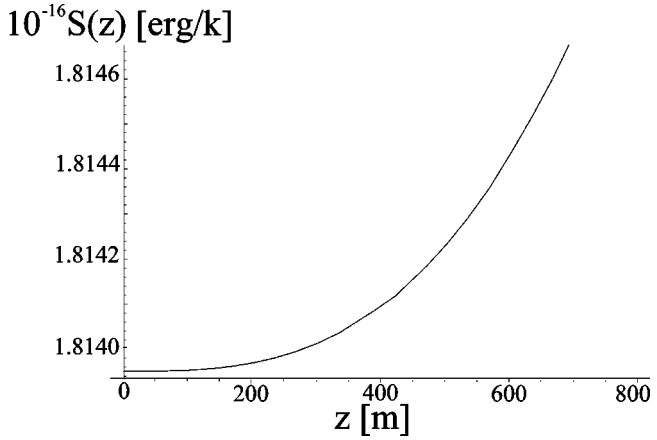


FIG. 6. The entropy of the system increases even if the error probability decreases in one quadrature with the length of the third-order nonlinear transmission line. Here $r_o^2=10$ and $\gamma/c=\chi/c=5\times10^{-5}$ m$^{-1}$.

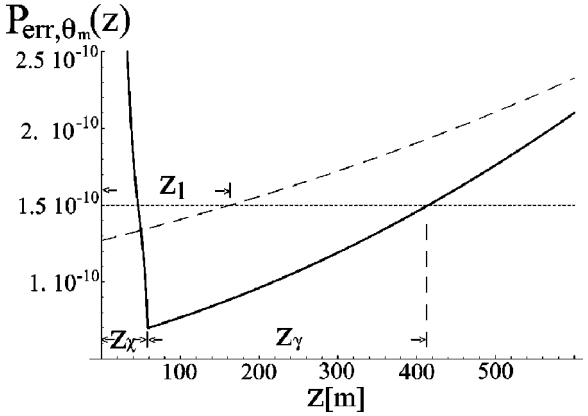


FIG. 7. The error function vs the length of propagation in two different media one followed by the other (continuous line), where the first is nonlinear and cut at $z_\chi=z_m$, while the second is linear. It is confronted with the error function in a linear medium (coarse grained dashed line). The accepted error probability (fine grained dashed line) is fixed at $P_{err}=1.5\times10^{-10}$. We observe a gain of the length of the transmission line. In the nonlinear-linear transmission line, the $\theta_m=20°$ quadrature is measured and in the linear fiber is measured the quadrature $\theta_m=0°$. Here $\chi/\gamma=10$, $\gamma/c=5\times10^{-5}$ m$^{-1}$, and $r_o^2=10$.

## IV. LONG HAUL TRANSMISSION

We can now think to an optical transmission line where a piece of nonlinear optical fiber is placed before the linear one, and we ask: how much longer could be this transmission line to have at the output the same error probability of a line made by a linear only medium? It is not possible to calculate such a quantity with the error function as in Eq. (5) because of the distribution at the input of the linear piece is no more Gaussian. The state of the quantum field, indeed, is not the coherent state because of the interaction with the nonlinear medium. It is then necessary to propagate the Wigner function, which we have at the end of the nonlinear piece, down the linear medium. This is possible by rewriting the Green function (17), then recalculating Eqs. (18), (19), (20), and (21) (see Appendix E). By measuring the quadrature $\theta_m=20°$ of the output field from the above optical line, with $r_o^2=10$, $\chi/c=10\gamma/c=10\gamma_\chi/c=5\times10^{-4}$ m$^{-1}$, where $\gamma_\chi/c$ the absorption coefficient for the nonlinear medium (i.e., we assume they have equal absorption), $z_\chi=59.26m$ and setting the maximally accepted error probability $P_{err}=1.5\times10^{-10}$ we obtain $z_\gamma=350m$. In the above expressions we have used $z_\chi$ and $z_\gamma$, respectively, for the length of the nonlinear fiber and the linear one, both having the same absorption coefficient. The same $P_{err}=1.5\times10^{-10}$ is obtained measuring the $\theta=0$ quadrature of the output field from the linear fiber with the same absorption coefficient as before but at a shorter length $z_l=160m$ (Fig. 7). Thus, with equal output error probability, we obtain a gain

$$G=\frac{z_\chi+z_\gamma}{z_l}=2.56, \tag{25}$$

equal to 4 dB. Whenever high nonlinear optical media will be available, it will be possible to think of transmission lines made of many pieces of nonlinear-linear media, thus improving the transmission more and more. Indeed, after the first linear piece, the distribution of fluctuations in phase space becomes almost uniform so that a new nonlinear interaction will produce another minimum. The error probability is calculated in the same way applying the Green function (5) many times and then Eqs. (18), (19), (20), and (21) (see Appendix E). The result is,

$$\begin{aligned}P_{err,\theta}(\zeta_N+\eta_N)=&\frac{1}{2}-\sqrt{\frac{2}{\pi}}r_o\exp[-(1/2)(\gamma_\chi\eta_N+\gamma\zeta_N)]\\&\times\sum_{m=1/odd}^{\infty}\frac{1}{m}\mathrm{Re}\Bigg(e^{im(\theta-\varphi_o)}[I_{(m-1)/2}\\&\times(-r_o^2\varepsilon_{N,m})-I_{(m+1)/2}(-r_o^2\varepsilon_{N,m})]\\&\times\exp\Bigg\{-r_o^2\Bigg[\varepsilon_{N,m}+\frac{im\chi}{\beta_m}\\&\times\sum_{k=1}^{N}(e^{-\beta_m t_{\chi_k}}-1)\varepsilon_{k-1,m}\Bigg]\Bigg\}\Bigg).\end{aligned} \tag{26}$$

where $\zeta_N=c\Sigma_{k=1}^N t_{\gamma_k}$ is the sum of the linear pieces with absorption coefficient $\gamma$, $\eta_N=c\Sigma_{k=1}^N t_{\chi_k}$ is the sum of the nonlinear ones with absorption $\gamma_\chi$ and $\varepsilon_{k,m}=\exp(-\beta_m\eta_k-\gamma\zeta_k)$ with $\gamma_\chi$ in $\beta_m$.

## V. CONCLUSIONS

We have shown that the error probability of bit transmission in an optical channel could be reduced even below the sender value, when a particular quadrature of the signal is measured at the output. This effect is interesting *per se* and is the manifestation of a quantum effect. In the classical case one could not observe the decreasing of error probability. In the quantum case one can have an enhancement of information in one particular quadrature with loss of information in

all other quadratures of the signal. This counter-intuitive result is a manifestation of the phase modulation due to the Kerr nonlinearity of the optical fiber and is not a mere consequence of squeezing. We have shown that to obtain this interesting result one should consider fibers with the ratio $\chi/\gamma$ of the order of the unity or even bigger. For the Kerr nonlinearity this requires $\chi^{(3)}\simeq 10^{-6}$ $m^2/V^2$ that is very high demanding when one considers the usual $SiO_2$ glass fibers with $\chi^{(3)}\simeq 4.5\times 10^{-20}$ $m^2/V^2$ [30]. However, many new materials are under consideration at present. In amorphous $Si/SiO_2$ superlatticies nonlinearities of $\chi^{(3)}\simeq 10^{-16}$ $m^2/V^2$ are reachable [31]. By using metal nanoclusters, obtained by implanting Ag ions in $LiNbO_3$, one obtains $\chi^{(3)}\simeq 10^{-14}$ $m^2/V^2$ [32], albeit the above high nonlinearities are obtained in a frequency range far from the fiber optics transmission frequency, which has a band width at *circa* 1560 nm with loss as small as 0.2 dB/km. A recent theoretical esteem in nonlinear periodic core waveguides gives $\chi^{(3)}\simeq 10^{-11}$ $m^2/V^2$ [15]. These values are still too far from the order of magnitude we need to obtain the above enhancement of transmission length at equal error probability. However, the search for higher $\chi^{(3)}$ nonlinearity is in progress and, hopefully, an increment of six order of magnitude could be obtained. If such a result could also be obtained at the frequency range of the usual optical fibers, the present proposal could have a great impact in the realization of long haul bits transmission with controllable error probability. The proposed scheme of multipieces transmission lines needs very low loss at the connections between linear and nonlinear pieces, i.e., the spline loss. One should, of course, consider fibers like the recently realized large effective area fibers, with the negligible spline loss of $6.8\times 10^{-3}$ dB [33].

## ACKNOWLEDGMENTS

Discussions with H. P. Yuen and A. Mecozzi are greatly acknowledged. C.F. acknowledges a grant from Guzzini S.P.A.

## APPENDIX A

Using the Caves and Crouch method [20], we start by calculating the constitutive relations for the electric field in terms of the displacement field **D** for a correct canonical approach [29]

$$E_{0s}^{(+)}=n_0^{-2}D_{0s}^{(+)}-3\pi n_0^{-8}\chi^{(3)}(D_{0s}^{(+)^2}D_{0s}^{(-)}+D_{0s}^{(+)}D_{0s}^{(-)}D_{0s}^{(+)}+D_{0s}^{(-)}D_{0s}^{(+)^2}), \tag{A1}$$

where for the symmetry of the nonlinear medium $\chi^{(3)}=\chi_{1111}$ and where $n(\omega)=n_0+\Delta n(\omega)$ is the frequency-dependent refraction index in the dispersive case. Now, from the Maxwell equations $c^{-1}\partial D_{0s}^{(+)}/\partial t=-\partial B_{0s}^{(+)}/\partial\xi$ and $\partial E_{0s}^{(+)}/\partial\xi=-c^{-1}\partial B_{0s}^{(+)}/\partial t$, it is possible to obtain the equation of motion for the quantum operators defining the positive components of the field on the spectrum of frequency $\mathcal{B}_s$ of width $\Delta_s$,

$$B_{0s}^{(+)}=\int_{\mathcal{B}_s}\frac{d\omega}{2\pi}B_{0s}(\omega,\xi)\exp[i(k_o\xi-\omega t)], \tag{A2}$$

and $k_0=\omega n_0/c$ while $B_{0s}(\omega,\xi)=(2\pi n_0\hbar\omega/c\sigma)^{1/2}a_{0s}(\omega,\xi)$. The absorption and dispersion are introduced by beams splitters between the slabs of nonlinear and ideal medium, assuming that the slabs are sufficiently thin we obtain the spatial differential equation for the signal

$$\begin{aligned}\frac{da_s(\omega,z)}{dz}=&-\frac{\gamma(\omega)}{2}a_s(\omega,z)+\sqrt{\gamma(\omega)}b_s(\omega,z)\\&-\frac{3i\chi^{(3)}\hbar}{4n_0\epsilon_0c^2\sigma}a_s(\omega,z)\int_{\mathcal{B}_s}d\omega'\,\omega'\\&\times\Bigg\{\Delta_s[\omega' a_s(\omega',z)a_s^+(\omega',z)\\&+\omega a_s^+(\omega',z)a_s(\omega',z)]+\int_{\mathcal{B}_s}d\omega''\sqrt{\frac{\omega''}{\omega'}}\\&\times[(2\omega'-\omega'')e^{ik(\omega',\omega'')z}a_s(\omega',z)a_s^+(\omega'',z)\\&+(\omega-\omega'+\omega'')e^{-ik(\omega',\omega'')z}\\&\times a_s^+(\omega',z)a_s(\omega'',z)]\Bigg\},\end{aligned} \tag{A3}$$

where $k(\omega',\omega'')=[\omega' n(\omega')-\omega'' n(\omega'')]/c$, and the noise operators $b_s(\omega,z)$ has the usual statistical properties as in Eq. (10). By considering a narrow bandwidth of frequencies $\Delta$ and defining $a(t,z)$ as

$$a(z,t)=\int_\Delta d\omega a_s(\omega,z)e^{i\omega t}, \tag{A4}$$

Eq. (A3) becomes

$$\begin{aligned}\frac{da(z,t)}{dz}=&-\frac{\gamma}{2}a(z,t)-i\frac{3}{2}\chi a(z,t)-i\chi a^+(z,t)a^2(z,t)\\&+\sqrt{\gamma}b(z,t),\end{aligned} \tag{A5}$$

where the second term of the right-hand side of Eq. (A5) is a linear phase factor and can be neglected for the evolution in one-mode propagation, by redefining the signal frequency. Now $\chi=3\chi^{(3)}\hbar\omega^2/2n_0\epsilon_0c^2\sigma$. Since $\Delta$ is small then the operator $a(z,t)\simeq a(z)$ is almost constant in time while the phase velocity is equal to the group velocity. Thus Eq. (A5) becomes

$$\frac{da(t)}{dt}=-\frac{c'\gamma}{2}a(t)-ic'\chi a^+(t)a^2(t)+c'\sqrt{\gamma}b(t), \tag{A6}$$

where $t=z/c'$ and $c'=c/n_o$. To obtain a ratio $\chi/\gamma=1$, with optical frequencies $\omega=10^{15}$ $s^{-1}$, $n_0=1.45$, and $\sigma=4\pi\times 10^{-12}$ $m^2$, we have to dispose of a fiber with a nonlinear susceptibility $\chi^{(3)}=4.5\times 10^{-6}$ $m^2/V^2$.

## APPENDIX B

Following the Kartner's and Schenzle's method [27] we set in their Eqs. (41), (42), and (43) the quantities $\kappa_m^0=(\gamma-im\chi)/\gamma$, $Q_m^0=(2\gamma-im\chi)/(4\gamma)$, $\lambda_{nm}^0=[\gamma\kappa_m^0(2n+|m|+1)-\gamma+2im\chi]/2$ and then write the Green function. To calculate the Wigner function with Eq. (16) it is necessary to know the initial function at $t=0$, in polar coordinates it can be expressed with the modified Bessel functions [27]

$$W(r,\varphi,0)=\frac{2}{\pi}e^{-2r^2-2r_o^2}\sum_{m=-\infty}^{\infty}I_m[4rr_o]e^{im(\varphi-\varphi_o)}, \tag{B1}$$

the angular part of the integral in Eq. (16) produce a Kronecker delta for the $m$'s indexes in both $G$ and $W(r,\varphi,0)$, the radial integral is of the form

$$\int_0^{\infty}e^{-ar^2}I_m[br]I_m[cr]rdr=\frac{1}{2a}\exp\left[\frac{b^2+c^2}{4a}\right]I_m\left[\frac{bc}{2a}\right], \tag{B2}$$

with $\mathrm{Re}[a]\geqslant 0$.

The integral in Eq. (14) is also of the same form and must be solved with the same procedure as well as for Eq. (19). Equation (20) is obtained by using Eq. (2) expressed in terms of Hermite polynomials

$$\langle\alpha|X_\theta\rangle=\sqrt[4]{\frac{2}{\pi}}\exp(-x^2/2-r^2/2)\sum_{n=0}^{\infty}\left[\frac{re^{i(\varphi+\theta)}}{\sqrt{2}}\right]^n\frac{H_n[x]}{n!}. \tag{B3}$$

The integrals on the angular parts still give the Kronecker delta that cancels two indexes, while it is necessary to expand the modified Bessel function in series to solve the radial part of the integral

$$I_m\{4r_oe^{-\beta_m t}\sqrt{r_1r_2}\exp[-i(\varphi_1-\varphi_2)/2]\}=\sum_{n=0}^{\infty}\frac{(2r_o\sqrt{r_1r_2}e^{-\beta_m t})^{m+2n}\exp[-i(m/2+n)(\varphi_1-\varphi_2)]}{n!(m+n)!}, \tag{B4}$$

obtaining

$$\int_0^{\infty}r^{2n+1}e^{-r^2}dr=\frac{n!}{2}. \tag{B5}$$

## APPENDIX C

Integrating by parts it is possible to obtain the integral recurrence formula,

$$\int_0^{\infty}e^{-x^2}H_n(x)H_k(x)dx=H_n(0)H_{k-1}(0)+2n\times\int_0^{\infty}e^{-x^2}H_{n-1}(x)H_{k-1}(x)dx, \tag{C1}$$

using $\int e^{-x^2}H_k(x)dx=-e^{-x^2}H_{k-1}(x)$ obtained from the definition of Hermite polynomials [28] and the property $H_n'(x)=2nH_{n-1}(x)$. We can now repeat the same procedure by interchanging the indexes of integrated functions

$$\int_0^{\infty}e^{-x^2}H_n(x)H_k(x)dx=H_{n-1}(0)H_k(0)+2k\times\int_0^{\infty}e^{-x^2}H_{n-1}(x)H_{k-1}(x)dx. \tag{C2}$$

Subtracting Eq. (C2) from Eq. (C1)

$$H_n(0)H_{k-1}(0)-H_{n-1}(0)H_k(0)+2(n-k)\times\int_0^{\infty}e^{-x^2}H_{n-1}(x)H_{k-1}(x)dx=0. \tag{C3}$$

Then increasing the indexes by one

$$\int_0^{\infty}e^{-x^2}H_n(x)H_k(x)dx=\frac{H_n(0)H_{k+1}(0)-H_{n+1}(0)H_k(0)}{2(n-k)}. \tag{C4}$$

Now, it is possible to use the formula $H_{2n}(0)=(-1)^n2^n(2n-1)!!$ and $H_{2n+1}(0)=0$ in the right-hand side of Eq. (C4) conveniently changing the indexes. The probability of error is

$$\begin{aligned}\int_{-\infty}^{0}dx|\langle X_\theta|\Psi(t)\rangle|^2&=\frac{1}{2}+\frac{r_oe^{-\gamma t}}{2\sqrt{2\pi}}\sum_{n,k=0}^{\infty}\frac{(-r_o/2e^{-\gamma t})^{n+k}}{n!k!}\\&\times\exp\{2i(n-k)[(n+k)\chi t-\theta]\}\\&\times\left(\frac{\exp\{i[(n+k)\chi t-\theta]-r_o^2f(n-k+1/2)\}}{n-k+1/2}\right.\\&\left.-\frac{\exp\{i[\theta-(n+k)\chi t]-r_o^2f(n-k-1/2)\}}{n-k-1/2}\right),\end{aligned} \tag{C5}$$

where $f(n-k\pm1/2)=(\gamma\exp\{-[\gamma-2i(n-k\pm1/2)\chi]t\}-2i(n-k\pm1/2)\chi)/[\gamma-2i(n-k\pm1/2)\chi]$. With some algebra and changing the index $n$ in $m=n-k$ it is possible to sum on $k$ in the modified Bessel functions to get

$$\int_{-\infty}^{0}|\langle X_\theta|\Psi(t)\rangle|^2dx$$
$$=\frac{1}{2}+\sqrt{\frac{2}{\pi}}r_o e^{-\gamma t}\sum_{m=-\infty}^{\infty}\frac{(-1)^m e^{-2im\theta}}{1-4m^2}$$
$$\times((m+1/2)\exp[i\theta-r_o^2 f(m-1/2)]$$
$$\times I_m\{r_o^2\exp[-\gamma t+2i(m-1/2)\chi t]\}-(m-1/2)$$
$$\times e^{-i\theta-r_o^2 f(m-1/2)}I_m\{r_o^2\exp[-\gamma t+2i(m+1/2)\chi t]\}). \tag{C6}$$

Changing the index $m$ in $2m+1$, i.e., summing only on odd $m$ and writing the first terms of the series for $m=-3,-1,1,3$, it is possible to collect the coefficients of the modified Bessel functions; observing at the end that for negative $m$ the terms of the series are the complex conjugate of terms with positive $m$ it is possible to obtain Eq. (21).

## APPENDIX D

For the entropy it is possible to calculate the trace of the density operator on the coherent states with the completeness relation

$$S(t)=-K_B Tr[\hat{\rho}(t)\ln\hat{\rho}(t)]$$
$$=-K_B\int\int\frac{d^2\alpha}{\pi}\frac{d^2\beta}{\pi}\langle\alpha|\hat{\rho}(t)|\beta\rangle\langle\beta|\ln\hat{\rho}(t)|\alpha\rangle, \tag{D1}$$

where $K_B$ is the Boltzman constant and the first expectation value is calculated in Eq. (19). For the second expectation value it is necessary to develop the log function and the binomial $(\hat{\rho}-1)^n$ in series [28]

$$\langle\beta|\ln\hat{\rho}(t)|\alpha\rangle=-\sum_{n=1}^{\infty}\frac{1}{n}\sum_{m=0}^{n}(-1)^m\binom{n}{m}\langle\beta|\hat{\rho}^m(t)|\alpha\rangle. \tag{D2}$$

With the completeness relation on the $\beta$ variables, and increasing the $m$ index by one we get

$$S(t)=-K_B\sum_{n=1}^{\infty}\frac{1}{n}\sum_{m=1}^{n+1}(-1)^m\binom{n}{m-1}\int\frac{d^2\alpha}{\pi}\langle\alpha|\hat{\rho}^m(t)|\alpha\rangle. \tag{D3}$$

The integral is transformed by using the completeness relation $m-1$ times and developing the modified Bessel function Eq. (19) in series. At this point it is possible to integrate the angular part to obtain Kronecker $\delta$ functions and obtain the same factorial for the integral of the radial part. For example, with the $m=3$

$$\mathrm{Tr}\,\hat{\rho}^3(t)=\sum_{k_1,k_2,k_3=0}^{\infty}\frac{(r_o^2e^{-\gamma t})^{k_1+k_2+k_3}}{\pi^3k_1!k_2!k_3!}$$
$$\times\exp\left\{-r_o^2\left[\frac{\gamma e^{-\beta_{k_2-k_1}t}-i(k_2-k_1)\chi}{\beta_{k_2-k_1}}\right.\right.$$
$$+\frac{\gamma e^{-\beta_{k_3-k_2}t}-i(k_3-k_2)\chi}{\beta_{k_3-k_2}}$$
$$\left.\left.+\frac{\gamma e^{-\beta_{k_1-k_3}t}-i(k_1-k_3)\chi}{\beta_{k_1-k_3}}\right]\right\}. \tag{D4}$$

Then, writing the general expression for any $m$ and substituting in Eq. (D3) we obtain the entropy

$$S(t)=-K_B\sum_{n=1}^{\infty}\frac{1}{n}\sum_{m=1}^{n+1}\left(\frac{-1}{\pi}\right)^m\binom{n}{m-1}$$
$$\times\sum_{k_1,\ldots,k_m=0}^{\infty}\frac{(r_o^2e^{-\gamma t})^{\sum_{j=1}^{m}k_j}}{\prod_{j=1}^{m}k_j!}\exp\left\{-r_o^2\right.$$
$$\times\left[\sum_{j=1}^{m-1}\frac{\gamma\exp(-\beta_{k_{j+1}-k_j}t)-i(k_{j+1}-k_j)\chi}{\beta_{k_{j+1}-k_j}}\right.$$
$$\left.\left.+\frac{\gamma e^{-\beta_{k_1-k_m}t}-i(k_1-k_m)\chi}{\beta_{k_1-k_m}}\right]\right\}. \tag{D5}$$

## APPENDIX E

Setting $\chi=0$ in the expression (17) and summing over $m$, we obtain the propagator for the Wigner function in a linear medium at time $t_\gamma$

$$G_\gamma(r,\varphi,t_\gamma;r',\varphi',0)=\frac{2}{\pi}\frac{1}{1-e^{-\gamma t_\gamma}}$$
$$\times\exp\left\{\frac{-2}{1-e^{-\gamma t_\gamma}}[r^2+r'^2e^{-\gamma t_\gamma}\right.$$
$$\left.-2rr'e^{-\gamma t_\gamma/2}\cos(\varphi-\varphi')]\right\}. \tag{E1}$$

The Wigner function is calculated starting from Eq. (19)

$$W(r,\varphi,t_\chi+t_\gamma)=\int_0^{2\pi}\int_0^{\infty}G(r,\varphi,t_\gamma;r',\varphi',0)W(r',\varphi',t_\chi)$$
$$\times r'dr'd\varphi'. \tag{E2}$$

Now repeating Eq. (E2) for more steps (nonlinear-linear) it is possible to obtain the Wigner function after the $N$'th step and then the probability distribution on the $X_\theta$ quadrature

$$|\langle X_\theta|\Psi(\zeta_N+\eta_N)\rangle|^2=\sqrt{\frac{2}{\pi}}e^{-2x^2}\sum_{n,m=0}^{\infty}\left(\frac{r_o^2\varepsilon_{N,n-m}}{2}\right)^{(n+m)/2}\exp\left[i(m-n)\left(\varphi_o-\theta+\frac{\chi}{2}\eta_N\right)\right]\frac{H_n[\sqrt{2}x]}{n!}\frac{H_m[\sqrt{2}x]}{k!}$$
$$\times\exp\left\{-r_o^2\left[\varepsilon_{N,n-m}+\frac{i(n-m)\chi}{\beta_{n-m}}\sum_{k=1}^{N}[e^{-\beta_{n-m}t_{\chi_k}}-1]\varepsilon_{k-1,n-m}\right]\right\}, \tag{E3}$$

where $t_{\gamma_0}=t_{\chi_0}=0$ and $\varepsilon_{0,n-m}=0$.


[1] R. W. Boyd, *Nonlinear Optics* (Academic Press, New York, 1992).
[2] C. W. Gardiner, *Quantum Noise* (Springer Verlag, 1991).
[3] P.D. Drummond *et al.*, Nature (London) **365**, 307 (1993).
[4] R. Loudon and P.L. Knight, J. Mod. Opt. **34**, 739 (1987).
[5] H.P. Yuen, Phys. Rev. A **13**, 2226 (1976).
[6] S.T. Ho *et al.*, Appl. Phys. Lett. **59**, 2558 (1991).
[7] S.R. Friberg, Appl. Phys. Lett. **63**, 429 (1993).
[8] A.M. Fox *et al.*, Phys. Rev. Lett. **74**, 1728 (1995).
[9] H. Schmidt and A. Imamoglu, Opt. Lett. **21**, 1936 (1996).
[10] S.E. Harris and L.V. Hau, Phys. Rev. Lett. **82**, 4611 (1999).
[11] G.I. Stegeman, M. Sheik-Bahae, E.V. Stryland, and G. Assanto, Opt. Lett. **18**, 13 (1993).
[12] G.I. Stegeman, J. Eur. Opt. Soc. Part B **9**, 139 (1997).
[13] L.V. Hau, S.E. Harris, Z. Dutton, and C.H. Behroozi, Nature (London) **397**, 594 (1999).
[14] M.M. Kash, V.A. Sautenkov, A.S. Zibrov, L. Hollberg, G.R. Welch, M.D. Lukin, Y. Rostovtsev, E.S. Fry, and M.O. Scully, Phys. Rev. Lett. **82**, 5229 (1999).
[15] S. She and S. Zhang, Opt. Commun. **161**, 141 (1999).
[16] A. Bohm, in *Quantum Mechanics* (Springer-Verlag, Berlin, 1993).
[17] E. Iannone, F. Matera, A. Mecozzi e M. Settembre, *Nonlinear Optical Communication Systems* (Wiley, New York, 1998).
[18] E. S. Ventsel, *Theorie Des Probabilites* (Mir, Moscow, 1978).
[19] A. Mecozzi and P. Tombesi, Opt. Commun. **75**, 256 (1990).
[20] C.M. Caves and D.D. Crouch, J. Opt. Soc. Am. B **4**, 1535 (1987).
[21] D. F. Walls and G. J. Milburn, *Quantum Optics* (Springer Verlag, Berlin, 1994).
[22] H.A. Haus and Y. Lai, J. Opt. Soc. Am. B **7**, 386 (1990).
[23] S.R. Friberg, S. Machida, M.J. Werner, A. Levanon, and Takaaki Mukai, Phys. Rev. Lett. **77**, 3775 (1996).
[24] A. Mecozzi and P. Kumar, Opt. Lett. **22**, 1232 (1997).
[25] D. Levandovsky, M. Vasilyev, and P. Kumar, Opt. Lett. **24**, 43 (1999).
[26] K.E. Cahill and R.J. Glauber, Phys. Rev. **177**, 1882 (1969).
[27] F.X. Kartner and A. Schenzle, Phys. Rev. A **48**, 1009 (1993).
[28] I. S. Gradshteyn and I. M. Ryzhik, Table of Integrals, Series, and Products (Academic Press, New York, 1994).
[29] M. Hillery and L.D. Mlodinow, Phys. Rev. A **30**, 1860 (1984).
[30] M. Asobe, T. Kanamori, and K. Kubodera, IEEE Photonics Technol. Lett. **4**, 362 (1992).
[31] N-N. Liu *et al.*, Opt. Commun. **176**, 239 (2000).
[32] S. Sarkisov *et al.*, Nucl. Instrum. Methods Phys. Res. B **141**, 294 (1998).
[33] S. Yi *et al.*, Opt. Commun. **177**, 225 (2000).